Atmospheric Environment 165 (2017) 359–369

Contents lists available at ScienceDirect

Atmospheric Environment

journal homepage: www.elsevier.com/locate/atmosenv

An example of aerosol pattern variability over bright surface using high resolution MODIS MAIAC: The eastern and western areas of the Dead Sea and environs

Lee Sever [a, b, *], Pinhas Alpert [c], Alexei Lyapustin [d], Yujie Wang [e], Alexandra Chudnovsky [b, f, **]

[a] Porter School of Environment, Tel Aviv University, Israel
[b] AIRO Lab, Department of Geography and Human Environment, Faculty of Exact Sciences, School of Geosciences, Tel-Aviv University, Israel
[c] Department of Geophysics, School of Geosciences, Tel Aviv University, Tel Aviv, Israel
[d] GEST / UMBC, NASA Goddard Space Flight Center, Baltimore, MD, USA
[e] University of Maryland, Baltimore County, Joint Center for Environmental Technology, Baltimore, USA
[f] Harvard T. H. Chan School of Public Health, Department of Environmental Health, Boston, MA, USA

HIGHLIGHTS

- Relatively good performance of MODIS MAIAC AOD retrievals over arid zones.
- Different AOD patterns emerged over the Dead Sea coasts.
- Western and eastern coasts showed seasonal dependence in aerosol concentrations.
- 'Rotem' industrial zone was clearly identified.

GRAPHICAL ABSTRACT

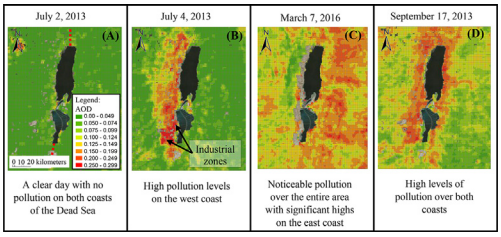

ARTICLE INFO

Article history:
Received 10 January 2017
Received in revised form
21 June 2017
Accepted 28 June 2017
Available online 29 June 2017

Keywords:
Aerosols
Aerosol optical depth (AOD)
MAIAC
MODIS
AERONET
The Dead Sea

ABSTRACT

The extreme rate of evaporation of the Dead Sea (DS) has serious implications for the surrounding area, including atmospheric conditions. This study analyzes the aerosol properties over the western and eastern parts of the DS during the year 2013, using MAIAC (Multi-Angle Implementation of Atmospheric Correction) for MODIS, which retrieves aerosol optical depth (AOD) data at a resolution of 1 km. The main goal of the study is to evaluate MAIAC over the study area and determine, for the first time, the prevailing aerosol spatial patterns. First, the MAIAC-derived AOD data was compared with data from three nearby AERONET sites (Nes Ziona - an urban site, and Sede Boker and Masada - two arid sites), and with the conventional Dark Target (DT) and Deep Blue (DB) retrievals for the same days and locations, on a monthly basis throughout 2013. For the urban site, the correlation coefficient (r) for DT/DB products showed better performance than MAIAC (r = 0.80, 0.75, and 0.64 respectively) year-round. However, in the arid zones, MAIAC showed better correspondence to AERONET sites than the conventional retrievals (r = 0.58–0.60 and 0.48–0.50 respectively). We investigated the difference in AOD levels, and its variability, between the Dead Sea coasts on a seasonal basis and calculated monthly/seasonal AOD averages for presenting AOD patterns over arid zones. Thus, we demonstrated that aerosol concentrations show a strong preference for the western coast, particularly during the summer season. This preference, is most likely a result of local anthropogenic emissions combined with the typical seasonal synoptic conditions, the Mediterranean Sea breeze, and the region complex topography. Our results also indicate that a large

* Corresponding author. Porter School of Environment, Tel Aviv University, Israel, AIRO Lab, Department of Geography and Human Environment, Department of Exact Sciences, Tel-Aviv University, Israel.
** Corresponding author. AIRO Lab, Department of Geography and Human Environment, Department of Exact Sciences, Tel-Aviv University, Israel.
E-mail addresses: lee_sever1@yahoo.co.uk (L. Sever), achudnov@post.tau.ac.il (A. Chudnovsky).

http://dx.doi.org/10.1016/j.atmosenv.2017.06.047

industrial zone showed higher AOD levels compared to an adjacent reference-site, i.e., 13% during the winter season.

1. Introduction

The Dead Sea region is the lowest place on earth, located at a height of approximately 430 m below sea level (BSL), and has unique climatic and landscape characteristics. Over the last 2000 years, the region has changed dramatically (Bookman et al., 2004; Kottmeier et al., 2012); suffering from an extreme rate of evaporation, the Dead Sea is drying out, and its surface level has dropped some 40 m in the last 40 years alone (Alpert et al., 1997; Shafir and Alpert, 2011). Furthermore, the Dead Sea area is characterized by a near-constant layer of haze owing to the extensive evaporation, which in turns leads to a more obstructed pathway for incoming solar radiation (Even-Paz and Shani, 1989). These conditions mean that the area is an important one for studying extreme aerosol pollution, which can reach a concentration of up to several thousand micrograms per cubic meter and have a negative impact on human health (Kishcha et al., 2016). On the extreme dust event of September 2015, concentrations reached a maximum of 1700–10,000 μg m-3 (based on three monitoring stations on the western side) (Alpert et al., 2016; Gasch et al., 2017; Mamouri et al., 2016), whereby the average annual value is around 50 μg m-3 (Kishcha et al., 2016).

The following factors influence aerosol dynamics in this region: 1) the very hot and dry climatic conditions (Shafir and Alpert, 2011); 2) large quantities of aerosols from different sources; 3) continual decline in the water level of the Dead Sea, which weakens the local Dead Sea breeze while intensifying the Mediterranean Sea breeze penetrating the valley (Shafir and Alpert, 2011); and 4) natural evapotranspiration of salts, bromine, and other minerals. Therefore, the study of aerosols in the Dead Sea can greatly enhance our understanding of extreme aerosol pollution and our ability to predict it.

Previous studies on the region's haze and dust aerosols have focused on a wide range of topics. Moore et al. (2013) studied spatial and temporal patterns of atmospheric mercury depletion events. Singer et al. both examined dust deposition using collectors installed at ground level (Singer et al., 2003), and the properties of suspended dust by means of direct sampling (Singer et al., 2004). Suspended atmospheric particles were also characterized by Kalderon-Asael et al. (2009). The vertical distribution of haze particles with regard to their physical and chemical properties was described by Levin et al. (2005). With other studies examining the relations between mineral dust aerosols and air quality (Ganor et al., 2009), the area's atmospheric optical depth and UVB irradiance components (Kottmeier et al., 2012), and the dust transport in the region by modeling (Vogel et al., 2006). However, to the best of our knowledge, no research has ever been conducted over the Dead Sea coasts to identify variability in aerosol levels. Furthermore, efforts to study this variability are hindered by the lack of ground monitoring data.

Satellite imagery is an important tool for evaluating air quality and pollution, owing to the extensive spatio-temporal monitoring of the earth surface and atmosphere (Kaufman et al., 2002; Kokhanovsky et al., 2007; Kaskaoutis et al., 2012). The main parameter derived from satellite observations for assessing air quality and atmospheric opacity is aerosol optical depth (AOD), a measure of the extinction of electromagnetic radiation at a given wavelength due to the presence of aerosols in an atmospheric column (Kaufman et al., 2002).

Since the Dead Sea is located in an arid zone, the bright arid areas surrounding it constitute a challenge for using remote sensing data due to the difficulty in discerning aerosols above the bright background terrains (Remer et al., 2005). With the release of the "Deep Blue" (DB) product, which is based on data from the 412 nm, 470 nm, and 670 nm spectral channels, it has become possible to study the spatial and temporal variability of transported dust/pollution over deserts, as bright surfaces show low reflectivity in the blue spectral region (Hsu et al., 2013). These data are available from the Sea-viewing Wide Field-of-view Sensor (SeaWiFS) (in operation from September 1997 to December 2010) and the Moderate Resolution Imaging Spectroradiometer (MODIS) (2000–current), which employ the DB algorithm (Hsu et al., 2004, 2006). Furthermore, the recent MODIS Collection 6 (C6) aerosol retrievals include enhanced 10 km DT and DB AOD and a "merged" DB-DT parameter at 10 km and 3 km resolutions (Levy et al., 2013; Hsu et al., 2013).

A Multi-Angle Implementation of Atmospheric Correction (MAIAC) algorithm (Lyapustin et al., 2011b) for MODIS provides a 1 km resolution aerosol retrieval. MAIAC has been shown to be successful in obtaining detailed AOD data over bright urban areas -in New England (Lee et al., 2011; Chudnovsky et al., 2013a, 2014), the southern United States (Lee et al., 2016), across the Mexico City metropolitan area (Just et al., 2015), and several regions in Israel (Kloog et al., 2015). MAIAC also has the novel ability to detect biomass burning (smoke) aerosol (Lyapustin et al., 2011b). The algorithm was tested in retrieving AOD in the European Alpine region, and showed good correlations (for MAIAC filtered data) with AERONET (AERosol Robotic NETwork) measurements (R ranging from 0.78 to 0.90) (Emili et al., 2011). Another advantage of MAIAC is its improved detection of cloudy and clear-sky areas, enabling it to produce AOD data over partially cloudy days, when the conventional 10 km resolution MODIS AOD returns no retrievals (Chudnovsky et al., 2013a, 2013b).

1.1. Problem definition: the need for high-resolution aerosol monitoring

With such extreme and rapid changes affecting the Dead Sea area, the environmental monitoring of aerosols is very important. As clearly seen in Fig. 1, the conventional MODIS aerosol product (a 10 km resolution) is insufficient for identifying aerosol patterns in this area. A solution may be offered by MAIAC (Panel B), which is able to retrieve data in this complex and ever-changing terrain, making it possible to identify variability in AOD patterns.

Given the challenges described above, the main goal of our study was to assess the accuracy of MAIAC over the Dead Sea coasts and, for the first time, determine the concentration patterns of aerosols in the region. To that end, the association between monthly data (January–December 2013) from MAIAC-derived AOD and from the three AERONET sites was investigated, and correlations to the conventional DT and DB retrievals for the same days and locations were calculated. In addition, we generated seasonal AOD maps and conducted a year-long study of the differences between AOD levels on the eastern and western coasts of the Dead

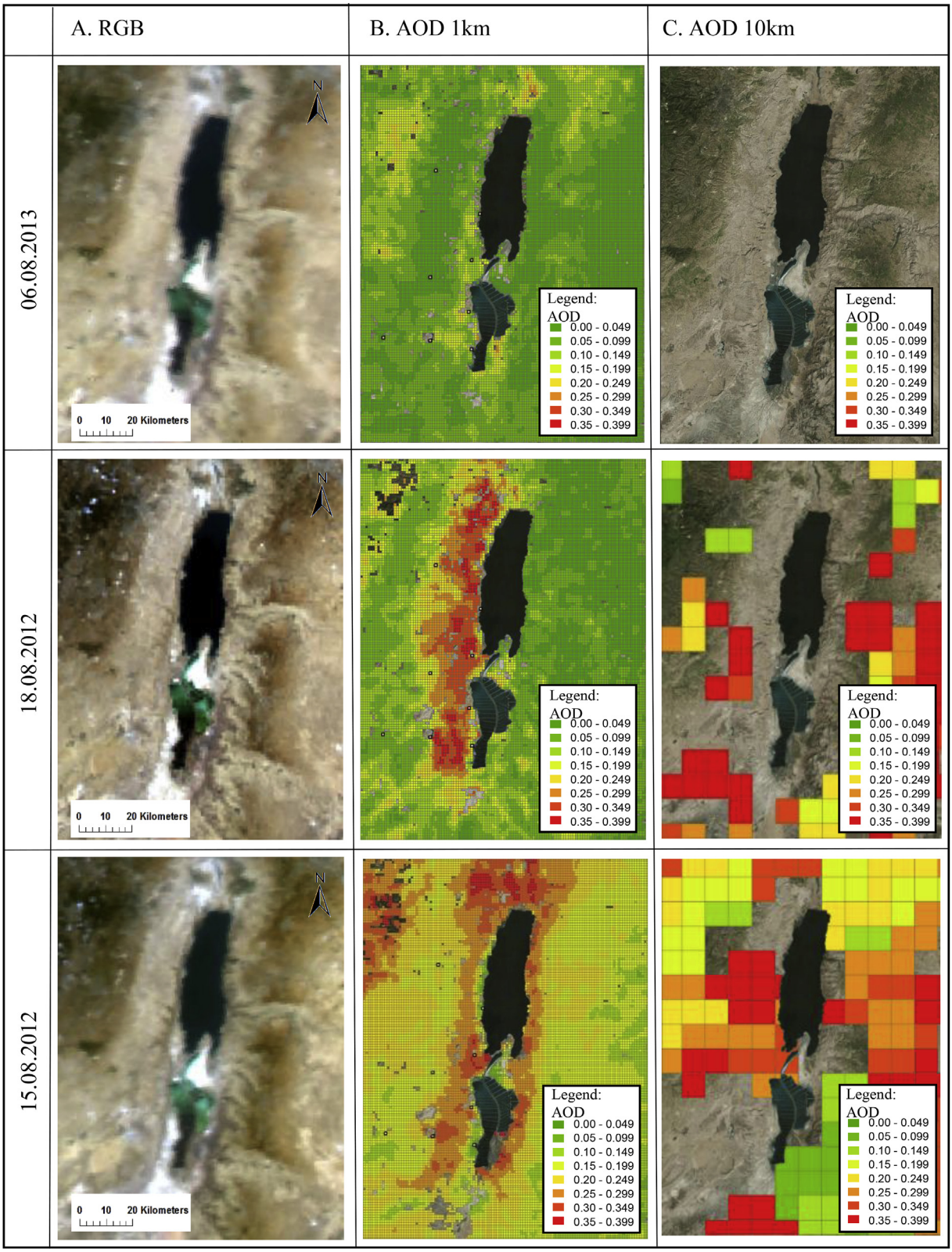

Fig. 1. AOD for selected days in August above the Dead Sea region. Panel A shows RGB data; Panel B shows MAIAC AOD data at a 1 km resolution; and Panel C shows MODIS Collection 6 combined (Dark Target + Deep Blue) AOD product. Note missing AOD values when compared to MAIAC. (For interpretation of the references to colour in this figure legend, the reader is referred to the web version of this article.)

Sea. This enabled us to identify distinct aerosol patterns over the Dead Sea coastal region. Finally, we compared differences in AOD levels between one of largest anthropogenic sources of pollution (Rotem factory) and a nearby reference site (each area consisting of 14 pixels).

2. Study area

The area chosen for this study comprises the land area immediately surrounding the Dead Sea. (The study of aerosols above the sea itself was excluded from the analysis due to an insufficient number of retrievals over the water). Hence, an area of roughly 120 km × 150 km was analyzed (Fig. 2).

In addition to the strip of hotels along the southern part of the sea, there are also several village/rural settlements and medium-sized cities in the region. The Dead Sea Works (potash plant) is located on the southwestern coast of the Dead Sea (at 390 m BSL), and the Rotem factory (400 m ASL), belonging to a large mining company that extracts phosphates from the Dead Sea and manufactures agricultural fertilizers and other chemical products, is found further to the west.

3. Material and methods

3.1. Satellite data

Our study relies on MAIAC AOD retrieval (at 470 nm) from the Aqua satellite MODIS (13:30 local time). MAIAC is an algorithm developed for MODIS that produces AOD data at a 1 km horizontal resolution (regardless of scanning angle) by using a time series of measurements from MODIS while simultaneously processing a group of pixels, with regional background models based on AERONET climatology (Lyapustin et al., 2011a). The aerosol retrieval procedure is based on the spectral similarity of the surface Bidirectional Reflectance Distribution Function (BRDF) shape between the visible (0.47 μm) and shortwave IR (2.13 μm) wavelengths, with look-up tables that contain pre-computed radiative transfer functions (Lyapustin et al., 2011a, 2011b, and 2012). Detailed information regarding MAIAC's radiative transfer basis and the look-up tables, aerosol algorithm, and atmospheric correction is described extensively by Lyapustin et al. (2011a, 2011b, and 2012) in a number of publications.

Cross-validation of MAIAC data with AERONET has showed MAIAC's high accuracy in retrieving AOD data over bright (urban)

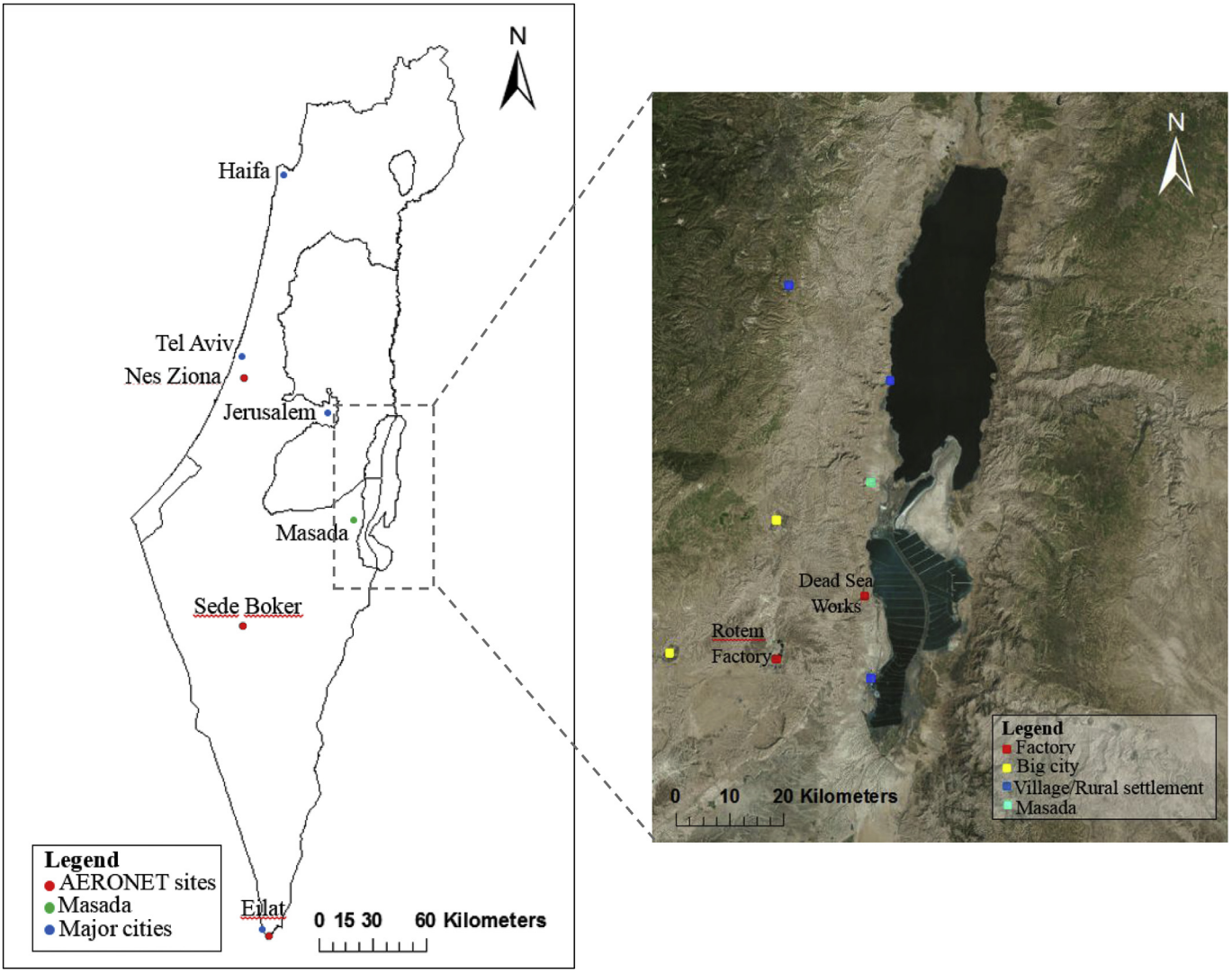

Fig. 2. Study Area. Left: a map of the area of Israel, with the Dead Sea region highlighted by the dotted line (major cities, AERONET stations, and Masada historical site marked); Right: an enlargement of the study area (rural settlements, cities, and industrial zones marked). The historical site of Masada is also marked.

surfaces in comparison with the standard MODIS AOD product (dark target algorithm), stemming from its more detailed surface characterization method (using surface BRDF rather than Lambertian reflectance model) and cloud detection (Lyapustin et al., 2011b). On the other hand, individual 1 km retrievals may sometimes have added noise, due to residual uncertainties in the surface reflectance or from cloud/snow contamination (Emili et al., 2011; Lyapustin et al., 2011a, 2011b; 2012).

In addition to MAIAC data, we used the Collection 6 combined aerosol product that includes Dark Target (DT) and Deep Blue (DB) AOD data for the period of 2013 at a spatial resolution of a 10 km × 10 km (at nadir). This product, over land and water, aims to fill the gaps in the three individual algorithms, creating a more complete picture of aerosols at 10 × 10 km resolution and at 550 nm (Sayer et al., 2014). Aqua MODIS C6 includes an operational combined AOD product calculated from DB and DT AOD in three Normalized Difference Vegetation Index (NDVI) categories (Hsu et al., 2006). This combined AOD is equal to DT AOD if NDVI >0.3 and is equal to DB AOD if NDVI <0.2. Detailed descriptions of the MODIS operational combined AOD algorithm and the QA flags can be found in Levy et al. (2013).

3.2. AERONET observations

Our analyses were geographically extended to include all available AERONET stations with high temporal resolution located in Israel (Fig. 1): the Nes Ziona station, located in an urban region (part of the Tel Aviv metropolis) at a height of about 40 m (ASL); the Sde Boker station, located in a kibbutz in the northern part of the Negev Region (an arid zone) at a height of 480 m ASL (this station is the closest one to the Dead Sea); and the Eilat station, located at the southernmost point of Israel, near the sea shore of Aqaba bay (also an arid zone) at a height of (15 m ASL).

The AOD values from the AERONET stations were chosen for the times correlating to the satellite passing over the region. Since not all AERONET AOD measurements were performed during the satellite pass time, eventually all analysis was conducted using the average AOD value of a 1-h time interval, from half an hour before the satellite pass to half an hour afterwards (13:30 ascending for Aqua). For each station, the AOD distribution was matched to the MAIAC AOD distribution, comparing the AOD value at the AERONET point location (a given latitude and longitude) to the AOD value of the MAIAC 1 km × 1 km pixel where the AERONET station was located. With regard to wavelength consistency, MAIAC provides AOT at 470 nm, where the retrievals are made, and at 550 nm for the users' convenience. In this work, AERONET AOT at 550 nm was obtained by linear interpolation which has a sufficient accuracy for this study. A higher accuracy could be obtained using second order interpolation (e.g., Eck et al., 1999).

3.3. Data processing and analysis: the methodological approach

Data processing was conducted in four major stages (Fig. 3). First, we have constructed a data base for analysis for the year 2013. All the retrievals from MAIAC were subjected to initial screening for days suitable for our study. AOD data for the three AERONET station located in Israel and for MODIS standard product was downloaded as well. All three data sources were combined to one data set by date. Second, in order to validate MAIACs quality of retrieval in the region, we have done a direct comparison of AERONET data to satellite-derived DT/DB and MAIAC data. Third, in order to identify seasonal differences in AOD concentration and patterns we have generated seasonal AOD maps. Next, we have compared aerosol pollution levels between the eastern and western areas of the Dead Sea. Lastly, we compared AOD levels between the large industrial zone of Rotem factory to a nearby reference site.

3.3.1. Data screening

All AOD retrieved images collected during 2013 were examined and compared to RGB images in order to identify cloudy days and days with unexplained missing data. This visual comparison was done since MAIAC have never been tested in the topographically complex region of the Dead Sea. To that end, a program in MATLAB language that opens and plots AOD and RGB images for each day simultaneously was written. This manual daily analyses for relatively new algorithms was also done by Ben-Ami et al. (2009) when CALIOP data was firstly released. Fig. 1s shows examples of days that were excluded from our analysis, and days that were eventually included in the analyses despite representing some inaccuracies. The most common reasons for disqualifying data (17% of the

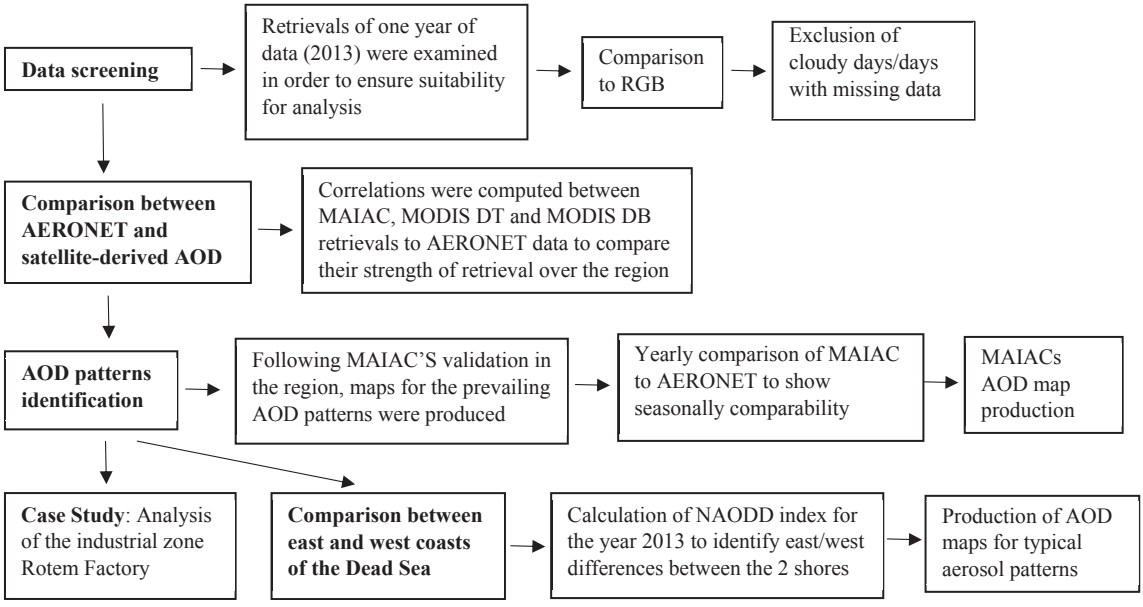

Fig. 3. Flow chart of the data analysis process.

sample in total was disqualified) were cloud cover (as in Panel B, for August 30, 2012) or missing AOD retrievals (as in Panel A, for August 3, 2012). In Panel A, we see clearly an area bordering the Dead Sea to the east (marked by a white circle) for which no data was retrieved and where no significant clouds were identified in the RGB image.

Data that exhibited residual calibration errors in the original MODIS L1B data, related to polarization effects (Franz et al., 2008), were included in our analyses. This phenomenon can be identified by parallel semi-horizontal stripes across the image. Sometimes these lines cannot be fully removed, even after a polarization correction is performed, as is demonstrated in Panel C of Fig. 1s (August 8, 2013).

3.3.2. AERONET vs satellite-derived AOD

Next, we investigated the associations between satellite-AOD and ground-based AERONET measurements (see Fig. 2 for AERONET station locations) for the year 2013. We made a comparison between Collection 6 DT, DBMYD04, and MAIAC retrievals for all available days on a seasonal basis. Following, we restricted our analyses to days when all retrievals were available for a given AERONET site (that is, same days and locations). Specifically, for the urban area we compared MAIAC, DB, and DT, whereas for the arid zone we compared MAIAC and DB.

In addition, we examined whether the relation between ground-based AERONET measurements and satellite AOD retrievals becomes stronger as the spatial resolution of the AOD becomes coarser. To that end, we used different spatial resolutions to determine what "box size" (representing a given number of pixels) would improve the correlation between MAIAC and AERONET measurements. The analysis was repeated for progressively degraded resolutions, from a 3 km × 3 km box (9 km^2), to a 5 km × 5 km box (25 km^2), and a 10 km × 10 km box (100 km^2), obtained from the original 1 km AOD data by simple averaging. Here we assumed that the coarser resolution can be adequately represented by a simple aggregation of the MAIAC fine resolution retrievals.

3.3.3. Seasonal spatial pattern and differences in aerosol levels between Dead Sea coasts

Following data screening, seasonal AOD averages were produced for all days that passed through our data quality test. Next, to capture the difference between two locations *i* and *k*, referred to as the Normalized AOD Difference (NAODD), we divided the difference in AOD values between both locations for the same days by the sum of their corresponding AODs, as follows:

$$NAODD = \left(AOD_{i,j} - AOD_{k,j}\right) / \left(AOD_{i,j} + AOD_{k,j}\right) \quad (1)$$

where j is the date of observation (that is, each point represents the calculated normalized difference on a given day).

Negative values of NAODD would correspond to days when location *k* is more polluted than location *i*, while values close to zero would correspond to days when pollution levels at locations *i* and *k* are similar, and high positive values would indicate days when location *i* is more polluted. Here, we compare between the eastern and western coasts of the Dead Sea. In addition, we compared between the Rotem factory site to a nearby reference location located at a height of 400 m above sea level. To that end, monthly average AOD was calculated for both locations. Here, only months with highest difference in average AOD values are reported.

4. Results

4.1. Direct comparison between DT/DB, MAIAC and AERONET retrievals

This section studies the subset of MYD04/MAIAC data for days when retrievals were available for a given AERONET site. Table 1 shows the comparison of AOD from AERONET with AOD from (MODIS) DT/DB and MAIAC in Israel (three locations) for 2013. As can be seen, the correlation varies by site. For the urban site, MAIAC shows slightly lower yearly correlations than DB/DT retrievals. Note that if dust storm days or "extreme points" were included, the correlations would have been similar and higher.

Table 2 shows a direct comparison between AOD from AERONET with DT/DB and MAIAC on a seasonal basis, for the same days in 2013 and the same three locations in Israel. While DT performs better in summer for the urban site, MAIAC is more accurate for the arid zone, producing better correlations there for all seasons except winter in Eilat.

4.2. AOD pattern

Fig. 4 shows monthly MAIAC and AERONET time-series measurements for the Sde Boker site during four representative

Table 1
Seasonal comparison between AERONET data and MODIS data (DT, DB, and MAIAC) for 2013 for the three AERONET satiations in Israel: Eilat, Sde Boker, and Nes Ziona.

Data source	Nes Ziona comparison – AERONET vs MODIS (DT, DB, MAIAC)					
	Statistics	Fall	Winter	Spring	Summer	Yearly
DT	N	28	22	34	48	132
	R	0.81	0.81	0.88	0.56	0.80
	Intercept	0.12	0.05	0.08	0.15	0.10
	Slope	0.56	1.10	1.08	0.74	0.91
DB	N	36	34	47	68	186
	R	0.53	0.68	0.86	0.39	0.75
	Intercept	0.07	0.07	0.06	0.11	0.02
	Slope	0.39	0.89	1.06	0.44	0.86
MAIAC	N	31	24	38	75	168
	R	0.80	0.77	0.6	0.53	0.64
	Intercept	0.02	0.07	0.08	0.04	0.06
	Slope	0.88	0.66	0.52	0.73	0.68
Data source	Sde Boker comparison – AERONET vs MODIS (DB, MAIAC)					
	Statistics	Fall	Winter	Spring	Summer	Yearly
DB	N	67	41	60	80	248
	R	0.26	0.27	0.62	0.27	0.51
	Intercept	0.23	0.21	0.30	0.38	0.28
	Slope	0.36	0.37	0.46	0.32	0.26
MAIAC	N	56	35	51	79	221
	R	0.64	0.60	0.57	0.79	0.60
	Intercept	0.03	0.03	0.11	0.03	0.09
	Slope	0.65	0.58	0.27	0.61	0.33
Data source	Eilat Comparison – AERONET vs MODIS (DB, MAIAC)					
	Statistics	Fall	Winter	Spring	Summer	Yearly
DB	N	26	14	53	52	145
	R	0.57	0.97	0.59	0.62	0.48
	Intercept	0.07	0.03	0.11	0.03	0.12
	Slope	0.25	0.53	0.24	1.18	0.29
MAIAC	N	23	11	50	58	142
	R	0.68	−0.15	0.65	0.66	0.58
	Intercept	0.11	0.17	0.19	0.11	0.17
	Slope	0.6	−0.11	0.20	0.76	0.25

Table 2
Seasonal comparison between DT/DB and MAIAC AOD for the same days and locations.

Data source	Season	Variable	DT	DB	MAIAC
Nes Ziona AERONET	Fall (N = 27)	R	0.57	0.47	0.59
		p-value	0.0016	0.047	0.0017
	Spring (N = 26)	R	0.478	0.439	0.62
		p-value	0.0009	0.0028	0.0009
	Summer (N = 44)	R	0.48	0.32	0.26
		p-value	0.006	0.0034	0.25
	Winter (N = 22)	R	0.94	0.87	0.88
		p-value	p < 0.0001	p < 0.0001	0.0001
Sde Boker AERONET	Fall (N = 61)	R	–	0.24	0.63
		p-value	–	0.063	p < 0.0001
	Spring (N = 53)	R	–	0.68	0.72
		p-value	–	p < 0.0001	p < 0.0001
	Summer (N = 84)	R	–	0.26	0.70
		p-value	–	p < 0.024	p < 0.0001
	Winter (N = 36)	R	–	0.27	0.56
		p-value	–	0.10	p < 0.0001
Eilat AERONET	Fall (N = 34)	R	–	0.29	0.75
		p-value	–	0.09	p < 0.0001
	Spring (N = 48)	R	–	0.47	0.67
		p-value	–	0.0007	p < 0.0001
	Summer (N = 51)	R	–	0.46	0.63
		p-value	–	0.0007	p < 0.0001
	Winter (N = 10)	R	–	0.11	−0.0059
		p-value	–	0.78	0.98

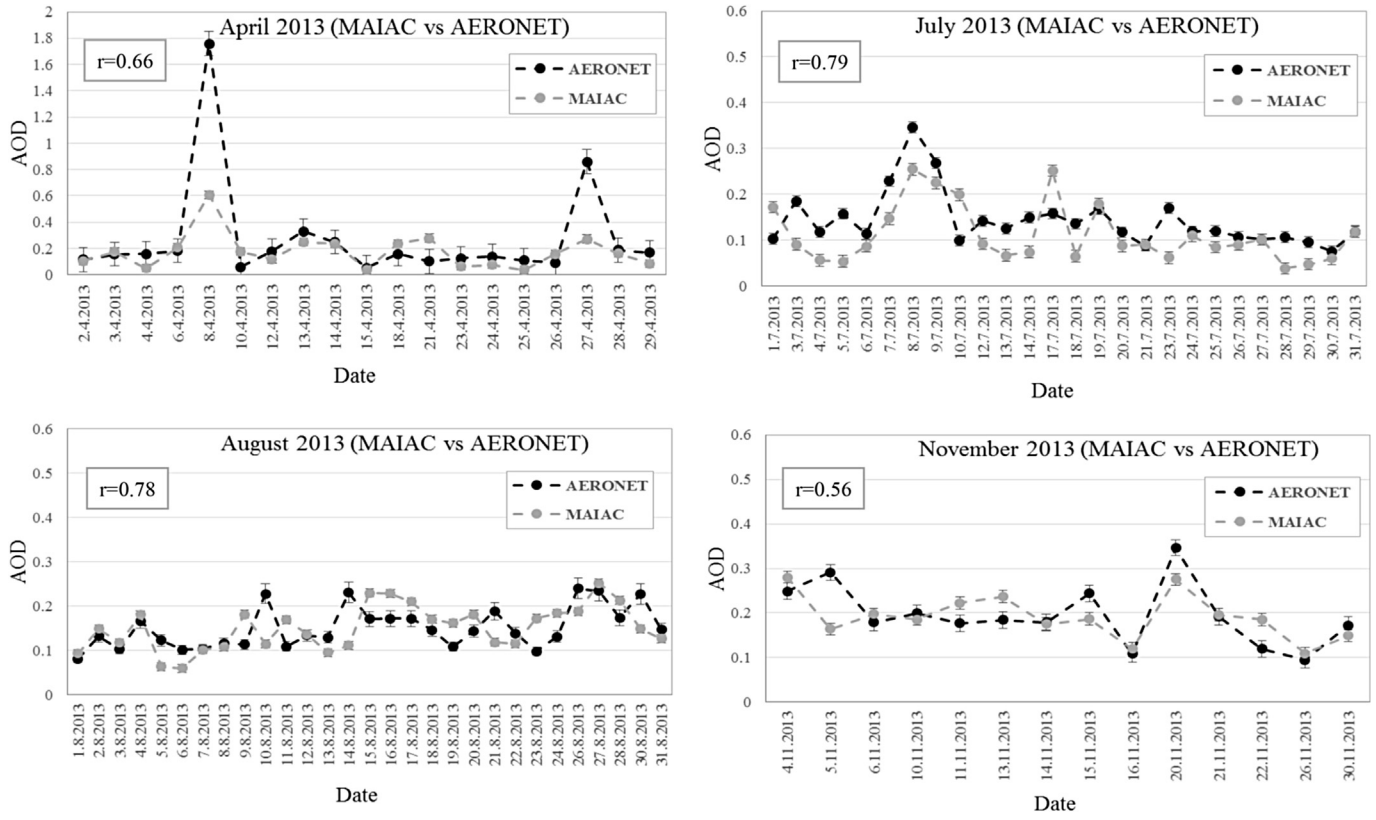

Fig. 4. Monthly trend of AOD for Sde Boker: Comparison between AERONET and MAIAC AOD retrievals. Error bars represent standard deviation.

months: April, July, August, and November 2013.

As can be seen, there are days when MAIAC overestimates or underestimates AOD compared to ground-based observations. However, the general monthly trend and variability of AOD from satellite-derived MAIAC are quite similar to those from AERONET. With this result in mind, we calculated seasonal means of AOD retrievals; these are presented in Fig. 5.

Fig. 5 shows the seasonal averages of MAIAC AOD for 2013. During spring, the dustiest season, there are higher AOD values over the entire region. The winter (December–February) and fall (September–November) months have a lower seasonal mean AOD, while during the summer we see a concentration of somewhat higher values around the western coast of the Dead Sea, where the northwestern wind penetrates the Negev, bringing humidity and

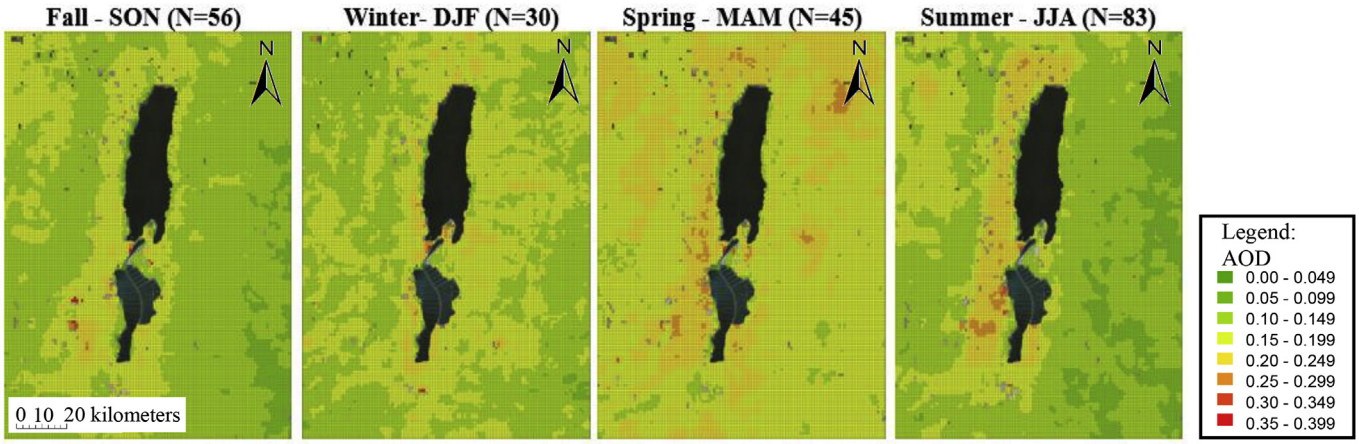

Fig. 5. Seasonal average of MAIAC AOD for 2013 (where N represents the number of available days for analysis in each season).

Table 3
Comparison of pollution levels between the eastern and western coasts of the Dead Sea for 2013, by season. Pollution focal, indicating the coast with the highest pollution on a given day, was determined by using the Normalized AOD difference index (NAODD). NAODD positive stands for higher aerosol levels above the east, while NAODD negative indicates higher aerosol levels over the western coast.

Season	Pollution focal: NAODD	Frequency	Percent (%)
Fall (77 days)	NAOOD>0 (East)	29	37.66
	NAOOD<0 (West)	48	62.34
Spring (67 days)	NAOOD>0 (East)	29	43.28
	NAOOD<0 (West)	38	56.72
Summer (91 days)	NAOOD>0 (East)	7	7.69
	NAOOD<0 (West)	84	92.31
Winter (45 days)	NAOOD>0 (East)	24	53.33
	NAOOD<0 (West)	21	46.67

air masses from the densely-populated industrial coast of central Israel as well as from Europe (Derimian et al., 2006). Previous studies has found that during this season and at this location, fine particle loadings with anthropogenic origin are dominant (Derimian et al., 2006; Dayan et al., 2017).

As shown in Fig. 1, during selected days in August, MAIAC exhibits high capability in retrieving AOD data over the bright arid area of the Dead Sea. This is apparent from the higher spatial coverage when comparing the algorithm to the conventional MODIS product. To further investigate the variability in AOD patterns over the region and their seasonal dependence, we calculated the NAODD (Normalized AOD Difference index) for 2013, and the results are shown in Table 3. As our results indicate, the western and eastern parts of the Dead Sea area have slightly different trends in NAODD values, lightly skewed toward positive values (that is, the west coast is more polluted). The 25th percentile is −0.22, the 50th percentile is 0.065, and the 75th percentile is 0.16, with a mean NAODD of 0.074.

On average, the western part of the Dead Sea has consistently higher aerosol concentration than the eastern side (Table 3). During the spring season (67 available days for analysis), more than half of the days in the sample (56.7%) exhibited higher AOD levels on the western coast. This percentage increased during the fall season (a sample of 77 days), where 62.3% of the days had higher AOD levels on the western side than on the east. This trend is seen at best during the summer season (91 days), when on 92.3% of the days, the aerosol-pollution levels were higher on the western side. During the winter, both coasts show similar AOD levels, with pollution being higher on the eastern/western side on 53.3/46.7% of the days, respectively. These results are not surprising and can be explained by the prevailing synoptic conditions in the region. In the summer, the Mediterranean Sea breeze is very strong on the western side and significantly weakens on the eastern side (Shafir and Alpert, 2011), which can explain the pronounced differences between the east and the west. In contrast, in the winter, the strong prevailing winds and the activity of the winter lows may create the observed similarity between the two coasts. While in the fall and spring intermediate synoptic conditions prevail.

Simulating the wind regime using the WRF model (three-dimensional scale), we found further explanation to our results (personal communication confirmed by numerical simulations, with Kunin, P., Rostkier-Edelstein, D., and Alpert, P.). The simulated local dynamics show the entrance of the Mediterranean Sea breeze at the western side, with a strong downward vertical velocity followed by a strong upward vertical wind, pertaining to the area topography. However, on the eastern side the upward motion is fairly weak. This wind dynamics was also discussed in the work of Bitan (1982), where he analyzed 10 years of data from 15 meteorological stations, and clearly identified the strong penetration of Mediterranean Sea breeze in the west during the summer (Fig. 2, in Bitan, 1982). Therefore, the wind regime described above bring about the strong local dust and aerosols emissions, with seasonal dependency which creates the pronounced differences between winter and summer. Several examples of days with variability in AOD levels between the two coasts are shown in Fig. 6.

Would a coarser resolution yield a better proxy for the AERONET observations measured at the ground? Here we assumed that perhaps the surface reflectance might have an impact on the accuracy of MAIAC AOD retrievals. The answer to our question is presented in Table 1s. As can be seen, the change in resolution does not affect the accuracy of urban Nes Ziona site, but does slightly improve the correlation for Sde Boker site. This result indicates that a coarser resolution contribute very little if at all to the improvement in the correlation between MAIAC and AERONET AOD measurements. Therefore we can not recommend using this tool as a standard procedure when anaylysing AERONET data, and its impact should be examined by site.

Finally, we compared between Rotem factory to a reference area with similar topographic conditions. Our results indicate that this large industrial zone showed higher AOD levels compared to an adjacent reference-site, i.e., 13% during the winter season. Other periods exhibited lower differences (April–May, 2–5% correspondingly) or even the opposite result (March).

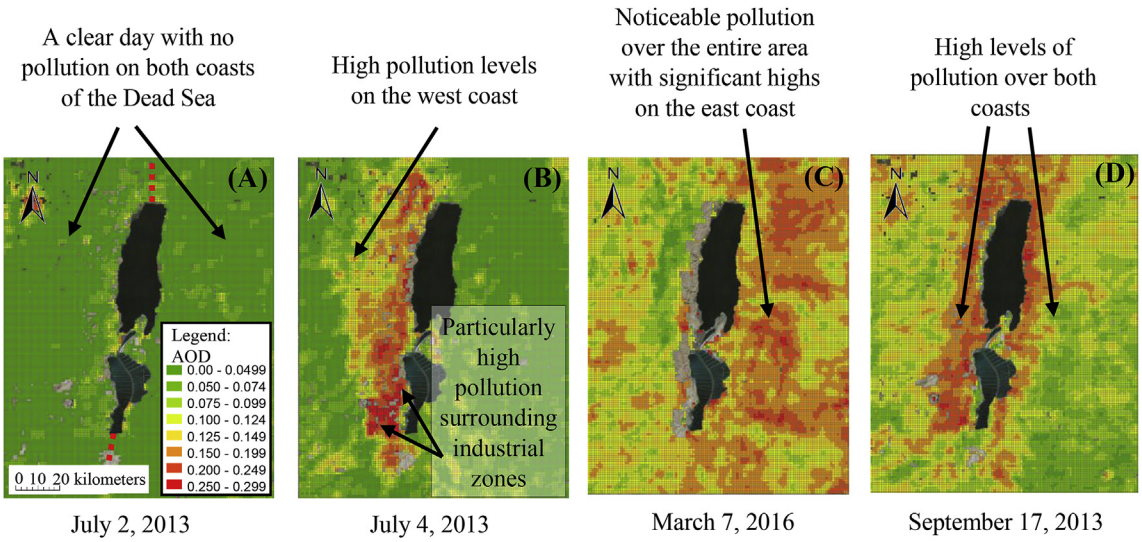

Fig. 6. AOD for selected days in above the Dead Sea region, each one representative of a different typical AOD pattern: (A) A clear day with hardly any aerosols over the region, on July 2, 2013 (the dotted line represents the division between the eastern and western parts of the Dead Sea region); (B) High AOD values concentrated along the west coast only (on July 4, 2013); (C) High AOD on the eastern side of the Dead Sea (March 7, 2016); and (D) elevated levels of aerosols above the entire region, with significantly higher aerosols concentration surrounding both eastern and western coasts of the Dead Sea (on the September 17, 2013).

5. Discussion

In this study, we examined the utility of MAIAC retrieval to assess the aerosols vertically-integrated concentration (AOD) over the arid region of the Dead Sea and the prevailing aerosol patterns. As seen in our presented results, the AOD patterns (Figs. 1 and 6) observed for the Dead Sea area not only indicate to the strength of MAIAC in retrieving data above bright reflecting regions, but also suggest that the region generates typical re-occurring patterns. In addition, there is a relatively good agreement between the MAIAC retrievals and AERONET measurements, as apparent from Fig. 4 for the nearby Sde Boker AERONET site.

The aerosol patterns seen over the Dead Sea region mostly show higher concentrations over the western part of the area compared to the eastern part, in particular during the summer season. This result is not surprising and can largely be explained by four main factors: (1) the unique synoptic and meteorological conditions; (2) the Mediterranean Sea breeze effect (Bitan, 1982; Kishcha et al., 2016; Alpert et al., 1997); (3) the breeze created by the Dead Sea itself; and (4) the areas unique topography and location (Bitan, 1974; and Bitan, 1977), as follows.

During the summer season, the persistent Persian Trough system cause local stability beneath the seasonal strong inversion layer at about 1 km above mean-sea-level. This allows the Mediterranean sea breeze to influence the area greatly alongside its unique topography, by enhancing the impact of local emission sources (Kishcha et al., 2016; Alpert et al., 1997; and Dayan et al., 2017) and transporting dust and anthropogenic aerosols from afar (Derimian et al., 2006, 2017). Specifically, Derimian et al. (2017) have shown that chemical composition, microphysical and optical properties of atmospheric aerosol deep inland in the Negev Desert of Israel were found to be influenced by daily occurrences of sea breeze flow from the Mediterranean Sea. A similar effect was described by Tokar et al. (1993), where authors demonstrated how pollution in Hadera (a coastal city in Israel) progresses inland due to this wind regime. During winter, however, strong winds and winter lows activity, contribute to stronger mixing and therefore yield to similar AOD levels on both coasts. It is interesting to note that a similar process was described for the region of lake Kinneret (the Sea of Galilee), roughly 120 km north to the Dead Sea along the Jordan Valley and 212 m BSL (Alpert et al., 1982). In this study, model simulation of the air flow in Lake Kinneret identified the strong entrance of the Mediterranean Sea breeze to the western shore of the lake, while on the eastern shore the winds were much weaker due to the unique topography of the area. This effect is caused by the interaction of the synoptic system with the meso-scale sea-breezes. The significant weakening on the eastern side does not evoke the same kind of emissions as showed by Kishcha et al. (2013, 2016, 2017).

The use of normalized AOD difference (NAODD index) made it possible to capture the seasonal variability in the aerosol levels between the eastern and western coasts of the Dead Sea. Mishra et al. (2014) studied aerosol properties over the eastern Mediterranean basin using a verity of techniques. They found that the summer 2010 AOD means are 0.22 ± 0.02 for polluted dust, 0.11 ± 0.04 for polluted continental, 0.10 ± 0.04 for dust, and 0.06 ± 0.01 for marine aerosol. In comparison, our results show that for the summer of 2013, the AOD mean was 0.17 ± 0.01 suggesting of polluted dust. In the future, adding ground monitoring stations would help to further validate our analyses. MODIS 3 km product should also be included for analyses and compared by means of spatial variability in AOD levels. Furthermore, additional research is required to improve the accuracy of the AOD estimates above desert regions such as the Middle East (Sayer et al., 2014 and De Meij and Lelieveld, 2011) and in other regions such as South and Southeast Asia (Kanniah et al., 2016).

Since our analysis pertained to one year, more data is required in order to fully understand the aerosol regime in the region, the prevailing aerosol patterns, and the atmospheric conditions that contribute to high aerosol concentrations. In addition, further research would be required in order to better understand the impact of the local industrial sources and their dynamics. In our study, we found that there is a “hot spot” area of higher AOD values surrounding the industrial region of Rotem factory (14 pixels, marked on Fig. 2), reaching a difference of 13% during the winter. Several studies examined the impact of local emissions in the New England Region of US (Tang et al., 2017; Schutgens et al., 2012). Unfortunately, no studies (to our knowledge) examined the impact

of local emissions or other anthropogenic activities, e.g. the role of land cultivation, population density, human activities and vehicle traffic, in the DS region. In this regard, MAIAC represents a strong data-base source for such endeavors. First, its high spatial coverage enables data analysis in areas with limited monitoring stations at ground level, e.g. the eastern shore of the Dead Sea. Second, its better resolution (1 × 1 km pixels) can identify local sources of pollution. Yet, this may mostly apply for cases with high and strong pollution emissions at the ground, which otherwise would have been significantly downgraded or gone unnoticed in lower resolution retrievals (i.e. MODIS standard10 × 10 km pixels). Chudnovsky et al. (2013a) have shown that fine resolution indicated spatial variability in particle concentration at a sub-10 km scale. Authors also found that the AOD coefficient of variation (CV), decreases as resolution coarsens.

To our knowledge, this is the first study that was able to show AOD patterns over the Dead Sea with such clarity. It should be noted that high resolution model results (1 km) to the region are not yet available. Kishcha et al. (2016) have conducted model simulations in the region for the March 2013 dust event, using the online-coupled weather forecast model COSMO-ART, with a grid of 0.025° (~3 km), identifying that the maximum near surface dust concentration was located on the western part of the valley. Yet this is a description of a singular event ('case study'), similar to the work of Gasch et al. (2017) (a grid of 2.5 km) and Alpert et al. (2016) (a ceilometer study) focusing on the September 2015 dust event. While our work has shown such a trend following a year of data analysis, which in turn allows us to classify climatological patterns.

Using both passive and active means of remote sensing at a high spatial and spectral resolution with angular observations above desert regions is the next step in improving current knowledge about dust and anthropogenic pollution. In this regard, the integration of a variety of satellite data on a pixel basis - combining data from passive systems such as OMI, MODIS, and VIIRS (which provide the spatial pattern of pollution) with data from active systems like CALIPSO (which provide information about the vertical distribution and classification of aerosols) - is required, given the close-knit relation between aerosol levels and atmospheric circulation, pollution sources, and radiation (e.g. Gkikas et al., 2016; Pappalardo et al., 2014; Thies and Bendix, 2011). Establishment of additional ground measurement sources such as ceilometers and Lidars will help to fully analyze the 3D aerosol regime in the DS area.

6. Concluding remarks

Until recently, the aerosol patterns above bright desert regions at high spatial resolution were unavailable. In this paper we used 1 km AOD retrieval from MODIS data based on the MAIAC algorithm and generated for the first time the prevailing aerosol spatial patterns above the Dead Sea coasts on a seasonal basis. These patterns are governed by the interaction of the synoptic system with the meso-scale sea-breezes and the region complex topography. Furthermore, we have shown that the high spatial resolution is essential to identify industrial zones/emissions as apparent from our preliminary analysis over Rotem factory.

Despite promising results, more data need to be processed and analyzed to understand the full potential and limitations of the high resolution MAIAC AOD product over bright desert regions. This will allow us to improve the accuracy in AOD retrieval and ground pollution level estimations and will greatly assist in future policy to preserve the unique Dead Sea area.

Acknowledgments

This research was supported by Grant Award No. RPGA 1501 from the Environment Health Fund (EHF), Israel. The German Helmholtz Association is gratefully acknowledged for (partly) funding this project within the Virtual Institute DESERVE (Dead Sea Research Venue) under contract number VH-VI-527. The authors also wish to extend gratitude to the reviewers. Their kind and insightful remarks, helped improve our paper greatly.

Appendix A. Supplementary data

Supplementary data related to this chapter can be found at http://dx.doi.org/10.1016/j.atmosenv.2017.06.047.

References

Alpert, P., Cohen, A., Neumann, J., Doron, E., 1982. A model simulation of the summer circulation from the eastern Mediterranean past lake Kinneret in the Jordan Valley. Mon. Weather Rev. 110, 106–118.
Alpert, P., Shafir, H., Issahary, D., 1997. Recent changes in the climate of the Dead Sea valley. Clim. Change 7, 1–25.
Alpert, P., Egert, S., Uzan, L., 2016. The 7-13 September extreme dust downfall over the East Mediterranean A two ceilometers study. In: EGU 5 General Assembly Conference Abstracts, vol. 18, p. 3788.
Ben-Ami, Y., Koren, I., Altaratz, O., 2009. Patterns of North African dust transport over the Atlantic: Winter vs. summer, based on CALIPSO first year data. Atmos. Chem. Phys. 9 (20), 7867–7875.
Bitan, A., 1974. The wind regime in the north-west section of the Dead Sea. Arch. Met. Geoph. Biokl 22 (Ser B), 313–335.
Bitan, A., 1977. The influence of the special shape of the Dead Sea and its environment on the local wind system. Arch. Met. Geoph. Biokl 24 (Ser B), 283–301.
Bitan, A., 1982. The Jordan Valley project - a case study in climate and regional planning. Energy Build. 4, 1–9.
Bookman, R., Enzel, Y., Agnon, A., Stein, M., 2004. Late holocene lake levels of the Dead sea. Geol. Soc. Am. Bull. 116, 555–571.
Chudnovsky, A., Kostinski, A., Lyapustin, A., Koutrakis, P., 2013a. Spatial scales of pollution from variable resolution satellite imaging. Environ. Pollut. 172, 131–138.
Chudnovsky, A., Tang, C., Lyapustin, A., Wang, Y., Schwartz, J., Koutrakis, P.A., 2013b. Critical assessment of high-resolution aerosol optical depth retrievals for fine particulate matter predictions. Atmos. Chem. Phys. 13 (21), 10907–10917.
Chudnovsky, A.A., Koutrakis, P., Kloog, I., Melly, S., Nordio, F., Lyapustin, A., Wang, Y., Schwartz, J., 2014. Fine particulate matter predictions using high resolution Aerosol Optical Depth (AOD) retrievals. Atmos. Environ. 89, 189–198.
Dayan, U., Ricaud, P., Zbinden, R., Dulac, F., 2017. Atmospheric pollution concentrations over the Eastern Mediterranean during summer - a review. Atmos. Chem. Phys. Discuss. http://dx.doi.org/10.5194/acp-2017-79.
De Meij, A., Lelieveld, J., 2011. Evaluating aerosol optical properties observed by ground-based and satellite remote sensing over the Mediterranean and the Middle East in 2006. Atmos. Res. 99, 415–433.
Derimian, Y., Karnieli, A., Kaufman, Y.J., Andreae, M.O., Andreae, T.W., Dubovik, O., Maenhaut, W., Koren, I., Holben, B.N., 2006. Dust and pollution aerosols over the Negev desert, Israel: properties, transport, and radiative effect. J. Geophys. Res. 111.
Derimian, Y., Choël, M., Rudich, Y., Deboudt, K., Dubovik, O., Laskin, A., Legrand, M., Damiri, B., Koren, I., Unga, F., Moreau, M., Andreae, M.O., Karnieli, A., 2017. Effect of sea breeze circulation on aerosol mixing state and radiative properties in a desert setting. Atmos. Chem. Phys. Discuss. http://dx.doi.org/10.5194/acp-2016-1084.
Eck, T.F., Holben, B.N., Reid, J.S., Dubovik, O., Smirnov, A., O'Neill, N.T., Slutsker, I., Kinne, S., 1999. Wavelength dependence of the optical depth of biomass burning, urban, and desert dust aerosols. J. Geophys. Res. 104 (1), 31333. http://dx.doi.org/10.1029/1999JD900923.
Emili, E., Lyapustin, A., Wang, Y., Popp, C., Korkin, S., Zebisch, M., Wunderle, S., Petitta, M., 2011. High spatial resolution aerosol retrieval with MAIAC: application to mountain regions. J. Geophys. Res. D23211.
Even-Paz, Z., Shani, J., 1989. The Dead Sea and psoriasis, Historical and geographic background. Int. J. Dermatol 28, 1–9.
Franz, B.A., Kwiatkowska, E.J., Meister, G., McClain, C.R., 2008. Moderate resolution imaging spectroradiometer on terra: limitations for ocean color applications. J. Appl. Remote Sens. 2, 023525. http://dx.doi.org/10.1117/1.2957964.
Ganor, E., Stupp, A., Alpert, P., 2009. A method to determine the effect of mineral dust aerosols on air quality. Atmos. Environ. 43, 5463–5468.
Gasch, P., Rieger, D., Walter, C., Khain, P., Levi, Y., Vogel, B., 2017. An analysis of the September 2015 severe dust event in the Eastern Mediterranean. Atmos. Chem. Phys. Discuss. http://dx.doi.org/10.5194/acp-2017-11.
Gkikas, A., Basart, S., Hatzianastassiou, N., Marinou, E., Amiridis, V., Kazadzis, S., Pey, J., Querol, X., Jorba, O., Gasśo, S., Baldasano, J.M., 2016. Mediterranean intense desert dust outbreaks and their vertical structure based on remote sensing data. Atmos. Chem. Phys. 16 (13), 8609–8642.
Hsu, N.C., Tsay, S.-C., King, M.D., Herman, J.R., 2004. Aerosol properties over bright-reflecting source regions. IEEE Trans. Geosci. Remot. Sen. 42, 557–569.

Hsu, N.C., Tsay, S.-C., King, M.D., Herman, J.R., 2006. Deep Blue retrievals of Asian aerosol properties during ACE-Asia. IEEE Trans. Geosci. Remot. Sen. 44 (11), 3180–3195. Art. no. 1717707.

Hsu, N.C., Jeong, M.-J., Bettenhausen, C., Sayer, A.M., Hansell, R., Seftor, C.S., Huang, J., Tsay, S.-C., 2013. Enhanced Deep Blue aerosol retrieval algorithm: the second generation. J. Geophys. Res. Atmos. 118 (16), 9296–9315.

Just, A.C., Wright, R.O., Schwartz, J., Coull, B.A., Baccarelli, A.A., Tellez-Rojo, M.M., Moody, E., Wang, Y., Lyapustin, A., Kloog, I., 2015. Using high-resolution satellite aerosol optical depth to estimate daily PM2.5 geographical distribution in Mexico City. Environ. Sci.Technol 49 (14), 8576–8584.

Kalderon-Asael, B., Erel, Y., Sandler, A., Dayan, U., 2009. Mineralogical and chemical characterization of suspended atmospheric particles over the east Mediterranean based on synoptic-scale circulation patterns. Atmos. Environ. 43 (25), 3963–3970.

Kanniah, K.D., Kaskaoutis, D.G., San Lim, H., Latif, M.T., Kamarul Zaman, N.A.F., Liew, J., 2016. Overview of atmospheric aerosol studies in Malaysia: known and unknown. Atmos. Res. 182, 302–318.

Kaskaoutis, D.G., Prasad, A.K., Kosmopoulos, P.G., Sinha, P.R., Kharol, S.K., Gupta, P., El-Askary, H.M., Kafatos, M., 2012. Synergistic use of remote sensing and modeling for tracing dust storms in the Mediterranean. Adv. Meteorology 2012, 14. http://dx.doi.org/10.1155/2012/861026. Article ID 861026.

Kaufman, Y., Tanré, D., Boucher, E., 2002. A satellite view of aerosols in the climate system. Nature 419, 215–223.

Kishcha, P., Starobinets, B., Udisti, R., Becagli, S., di Sarra, A., Nickovic, S., Alpert, P., 2013. Sea-salt aerosol forecasts over the Mediterranean Sea evaluated by daily measurements in Lampedusa from 2006 to 2010. NATO Sci. Peace Secur. Ser. C: Environ. Secur. 137, 321–322.

Kishcha, P., Rieger, D., Metzger, J., Starobinets, B., Bangert, M., Vogel, H., Schäettler, U., Corsmeier, U., Alpert, P., Vogel, B., 2016. Modeling of a strong dust event in the complex terrain of the Dead Sea valley during the passage of a gust front. Tellus, Ser. B:Chem. Phys. Meteorol. 68 (1) art. no. 29751.

Kishcha, P., Starobinets, B., Savir, A., Alpert, P., Kaplan, M., 2017. Foehn-induced effects on local dust pollution, frontal clouds and solar radiation in the Dead Sea valley. Meteorol. Atmos. Phys. 1–15.

Kloog, I., Sorek-Hamer, M., Lyapustin, A., Coull, B., Wang, Y., Just, A.C., Schwartz, J., Broday, D.M., 2015. Estimating daily PM2.5 and PM10 across the complex geo-climate region of Israel using MAIAC satellite-based AOD data. Atmos. Environ. 122, 409–416.

Kokhanovsky, A., Breon, F.-M., Cacciari, A., Carboni, E., Diner, D., Di Nicolantonio, W., Grainger, R., Grey, W., Höller, R., Lee, K.-H., Li, Z., North, P., Sayer, A., Thomas, G., von Hoyningen-Huene, W., 2007. Aerosol remote sensing over land: a comparison of satellite retrievals using different algorithms and instruments. Atmos. Res. 85, 372–394.

Kottmeier, C., Agnon, A., Al-Halbouni, D., Alpert, P., Corsmeier, U., Dahm, T., Eshel, A., Geyer, S., Haas, M., Holohan, E., Kalthoff, N., Kishcha, P., Krawczyk, C., Lati, J., Kudish, A., Evseev, E., 2012. UVB irradiance and atmospheric optical depth at the Dead Sea basin, Israel: measurements and modeling. Renew. Energ 48, 344–349.

Lee, H.J., Liu, Y., Coull, B.A., Schwartz, J., Koutrakis, P., 2011. A novel calibration approach of MODIS AOD data to predict PM2.5 concentrations. Atmos. Chem. Phys. 11 (15), 7991–8002.

Lee, M., Kloog, I., Chudnovsky, A., Lyapustin, A., Wang, Y., Melly, S., Coull, B., Koutrakis, P., Schwartz, J., 2016. Spatiotemporal prediction of fine particulate matter using high resolution satellite images in the southeastern U.S 2003-2011. J. Exp. Sci. Env. Epid 26 (4), 377–384.

Levin, Z., Gershon, H., Ganor, E., 2005. Vertical distribution of physical and chemical properties of haze particles in the Dead Sea valley. Atmos. Environ. 39, 4937–4945.

Levy, R.C., Mattoo, S., Munchak, L.A., Remer, L.A., Sayer, A.M., Patadia, F., Hsu, N.C., 2013. The Collection 6 MODIS aerosol products over land and ocean. Atmos. Meas. Tech. 6 (11), 2989–3034.

Lyapustin, A., Martonchik, J., Wang, Y., Laszlo, I., Korkin, S., 2011a. Multiangle implementation of atmospheric correction (MAIAC): 1. Radiative transfer basis and look-up tables. J. Geophys. Res. 116, D03210.

Lyapustin, A.I., Wang, Y., Laszlo, I., Kahn, R.A., Korkin, S., Remer, L.A., Levy, R.C., Reid, J., 2011b. Multiangle implementation of atmospheric correction (MAIAC): 2. Aerosol algorithm. J. Geophys. Res. 116 (D3) http://dx.doi.org/10.1029/2010JD014986. D03211.

Lyapustin, A., Wang, Y., Laszlo, I., Hilker, T., Hall, F., Sellers, P., Tucker, C., Korkin, S., 2012. Multiangle implementation of atmospheric correction (MAIAC): 3. Atmospheric correction. Remote Sens. Environ. 127, 385–393.

Mamouri, R.E., Ansmann, A., Nisantzi, A., Solomos, S., Kallos, G., Hadjimitsis, D.G., 2016. Extreme dust storm over the eastern Mediterranean in September 2015: satellite, lidar, and surface observations in the Cyprus region. Atmos. Chem. Phys. 16, 13711–13724. http://dx.doi.org/10.5194/acp-16-13711-2016.

Mishra, A.K., Klingmueller, K., Fredj, E., Lelieveld, J., Rudich, Y., Koren, I., 2014. Radiative signature of absorbing aerosol over the eastern Mediterranean basin. Atmos. Chem. Phys. 14 (14), 7213–7231.

Moore, C.W., Obrist, D., Luria, M., 2013. Atmospheric mercury depletion events at the Dead Sea: spatial and temporal aspects. Atmos. Environ. 69, 231–239.

Pappalardo, G., Amodeo, A., Apituley, A., Comeron, A., Freudenthaler, V., Linné, H., Ansmann, A., Bösenberg, J., D'Amico, G., Mattis, I., Mona, L., Wandinger, U., Amiridis, V., Alados-Arboledas, L., Nicolae, D., Wiegner, M., 2014. EARLINET: towards an advanced sustainable european aerosol lidar network. Atmos. Meas. Tech. 7 (8), 2389–2409.

Remer, L., Kaufman, Y., Tanré, D., Mattoo, S., Chu, D., Martins, J., Li, R.-R., Ichoku, C., Levy, R., Kleidman, R., Ect, T., Vermote, E., Holben, B., 2005. The MODIS aerosol algorithm, products and validation. J. Atmos. Sci. 62, 947–973.

Sayer, A., Munchak, L., Hsu, N., Levy, R., Bettenhausen, C., Jeong, M.-J., 2014. MODIS Collection 6 aerosol products: comparison between Aqua's e-Deep Blue, Dark Target, and "merged" data sets, and usage recommendations. J. Geophys. Res. Atmos. 119, 13,965–13,989.

Schutgens, N., Nakata, M., Nakajima, T., 2012. Estimating aerosol emissions by assimilating remote sensing observations into a global transport model. Remote Sens. 4 (11), 3528–3543.

Shafir, H., Alpert, P., 2011. Regional and local climatic effects on the Dead-Sea evaporation. Clim. Change 105, 455–468. http://dx.doi.org/10.1007/s10584-010-9892-8.

Singer, A., Ganor, E., Dultz, S., Fischer, W., 2003. Dust deposition over the Dead sea. J. Arid. Environ. 53, 41–59.

Singer, A., Dultz, S., Argaman, E., 2004. Properties of the non-soluble fractions of suspended dust over the Dead Sea. Atmos. Environ. 38, 1745–1753.

Tang, C.-., Coull, B.A., Schwartz, J., Lyapustin, A.I., Di, Q., Koutrakis, P., 2017. Developing particle emission inventories using remote sensing (PEIRS). J. Air Waste Manag. Assoc. 67 (1), 53–63. http://dx.doi.org/10.1080/10962247.2016.1214630.

Thies, B., Bendix, J., 2011. Satellite based remote sensing of weather and climate: recent achievements and future perspectives. Met. Apps 18, 262–295. http://dx.doi.org/10.1002/met.288.

Tokar, Y., Goldstein, J., Levin, Z., Alpert, P., 1993. The use of a meso-gamma scale model for evaluation of pollution concentration over an industrial region in Israel (Hadera). Bound. Lay. Meteor. 62, 185–193.

Vogel, B., Hoose, C., Vogel, H., Kottmeier, C., 2006. A model of dust transport applied to the Dead Sea area. Meteorol. Z. 15, 611–624.